Structural Engineering and Mechanics, Vol. 16, No. 2 (2003) 195-217
DOI: http://dx.doi.org/10.12989/sem.2003.16.2.195

Effect of boundary conditions on the stability of beams under conservative and non-conservative forces

Alessandro Marzani†

Department of Structures, University of Calabria, via Pietro Bucci, Arcavacata di Rende Cosenza, Italy

Erasmo Viola‡

Department of Civil Engineering, DISTART, University of Bologna, Viale Risorgimento 2, Bologna, Italy

(Received February 15, 2003, Accepted May 26, 2003)

Abstract. This paper, which is an extension of a previous work by Viola *et al.* (2002), deals with the dynamic stability of beams under a triangularly distributed sub-tangential forces when the effect of an elastically restrained end is taken into account. The sub-tangential forces can be realised by a combination of axial and tangential follower forces, that are conservative and non-conservative forces, respectively. The studied beams become unstable in the form of either flutter or divergence, depending on the degree of non-conservativeness of the distributed sub-tangential forces and the stiffness of the elastically restrained end. A non-conservative parameter α is introduced to provide all possible combinations of these forces. Problems of this kind are usually, at least in the first approximation, reduced to the analysis of beams according to the Bernoulli-Euler theory if shear deformability and rotational inertia are negligible. The equation governing the system may be derived from the extended form of Hamilton's principle. The stability maps will be obtained from the eigenvalue analysis in order to define the divergence and flutter domain. The passage from divergence to flutter is associated with a noticeable lowering of the critical load. A number of particular cases can be immediately recovered.

Key words: dynamic instability; non-conservativeness; sub-tangential forces; flutter and divergence; elastically restrained end.

1. Introduction

The analysis of the statics, the dynamics and particularly of the stability of columns under a non-potential load occupies a lot of space in the literature. Recently, a considerable amount of works has been published on the problem of elastic stability of a structural system under the action of non-conservative sub-tangential forces which are of particular importance in modern engineering practice. The sub-tangential forces are the combination of the axial forces and the tangential follower forces. As is well known, the axial forces satisfy the principle of conservation of energy, and their work over any admissible displacements of the body is path-independent. In fact, the axial

† PhD Student
‡ Full Professor of Structural Mechanics

forces always act in the same direction so they are conservative, i.e. derivable from a potential function. The tangential follower forces, instead, are dependent on the deformation of the body on which they act and are non-conservative, i.e. not derivable from a potential function. However, they can still be defined by the work done over an arbitrary small displacement. In literature these types of systems may be called “Hybrid-type system”, because their loss of stability occurs through divergence or flutter depending on the degree of the non-conservativeness of the load (Argyris and Symeonidis 1981). It is known that if the type of instability is divergence, the critical loads of the system can be determined by a static approach, while for flutter the critical loads should be determined using the dynamic criterion.

From a mathematical point of view some differences exist between conservative and non-conservative stability problems. The mathematical treatment of conservative stability problems leads to the analysis of self-adjoint boundary eigenvalues problem. The respective eigenvalues are real and can be established by employing the static stability criterion; moreover, they are positive and simple, forming, when ordered with respect to the magnitude, a denumerable infinite sequence associated with corresponding eigenfunctions which constitute a complete orthogonal system. An essentially different mathematical structure presents the problem of stability of non-conservative systems. In fact, the differential equations governing the equilibrium of these systems are not self-adjoint. The eigenvalues of the above non self-adjoint problems may be real or complex. In the first case the static stability criterion is applicable and the instability of the system is in the form of the divergence, whereas in the second case, that of flutter instability, it cannot be employed. Application of the dynamic stability criterion entails increased computational work.

In a finite element formulation, the analysis of a geometrically non-linear elastic system subject to such non-conservative forces gives rise, in general, to a contributory non-symmetric stiffness matrix known as the load correction matrix. As a result, the total tangent stiffness matrix becomes non-symmetric, an indication of the non self-adjoint character of the problem, and the corresponding eigenvalues problem can exhibit complex eigenvalues. It should be noted that, owing to the action of the non-conservative forces applied to a beam, the system undergoes a deformation which may be mathematically described by a deflection vector. This vector has one predominant component: the lateral deflection of the beam. The instability of the system occurs for the critical values of the loads under which the deflection vector may become unbounded. Since the transition of the beam from the state of equilibrium to the state of instability is always related to a motion, it is appropriate to use the dynamic analysis for the investigation of this transition and to discuss in which way the stability is lost.

Early studies regarding the non-conservative system have been carried out starting in the second half of the twentieth century. In the first place the inadequacy of the static criterion, also called Euler method, was recognised. One of the simplest non-conservative problems is the cantilevered beam subjected to an end tangential follower force, known as Beck’s column (Beck 1952). About twenty five years later, Ziegler (1977) was the first to apply the dynamic criterion to the instability problem of non-conservative systems and found the flutter load value for Beck’s column. Many investigations have been devoted to the determination of the influence of parameters on the values of the critical flutter load of non-conservatively loaded elastic system. In books by (Bolotin 1965), (Leipholz 1980) and (Ziegler 1977), these problems and various types of non-conservative forces often encountered in practical engineering design are well discussed and illustrated. In the study of non-conservative systems, the non-conservative parameter was introduced to provide a smooth transition from the fixed loading to the follower loading.

Some authors have investigated the stability of elastic column under a various combination of axial and tangential forces. Leipholz and Bhalla (1977) presented an exact method for solving stability problem of columns subjected to triangularly distributed tangential forces. It was found that the systems lose their stability by divergence or flutter depending on the distribution pattern of the loading, as well as the boundary conditions. Sugiyama and Kawagoe (1975) first, and Sugiyama and Mladenov (1983) later, introduced a uniform and triangular distribution of sub-tangential follower forces, respectively, thus filling the gap between the classical conservative and purely circulatory cases.

With the advances in computer hardware and software, numerical methods have become popular for analysing the stability of non-conservatively systems. Of the numerical methods, the most commonly employed is the finite element method. Mote (1971) presented the finite element procedure and solution technique for various elastic system. Kounadis (1983) investigated the existence of regions of divergence instability for an elastically restrained column under a concentrated follower force. Lee (1995), by using the finite element method, analysed the stability of the column subjected to sub-tangential follower forces, while Ryu *et al.* (2000) performed a vibration and stability analysis of a column clamped at one end and elastically supported at an arbitrary location, subjected to triangularly distributed sub-tangential forces. The influence of an intermediate support on the stability behaviour of cantilever beams subjected to follower force was also studied by De Rosa and Franciosi (1990). Glabisz (1999) presented an exact algorithm for the determination of the free vibration frequency of beam systems under conservative and non-conservative forces for various boundary conditions. However, as far as the authors know, there are no papers dealing with beams having general elastic boundary conditions at their ends under a distributed sub-tangential follower forces.

In this paper, it will be shown that for certain intervals of the values of the parameters of the elastic end constraints, these structures are of the divergence type, whereas outside these regions they are of the flutter type. At the boundaries of the region, where the buckling mechanism changes from divergence to flutter or from flutter to divergence, a sudden jump in the critical load has been observed. Moreover, a thorough discussion of the influence of the aforementioned stiffness parameter on the type of instability and the smallest eigenvalue of an elastically restrained column under a triangularly distributed sub-tangential forces, is performed using the dynamic stability criterion. In addition, the variation of the critical load and the frequencies of the column have been explored for various boundary conditions at the ends of the beam, where an elastic constraint and one non-elastic constraint can take place. Many other results are reported by Viola and Marzani (2002).

The present paper is organised as follows. In section 2, the statement of the problem and the calculation of the energetic terms to obtain the motion equation are detailed. In section 3, the finite element formulation is derived. In section 4, the numerical results are discussed and graphically illustrated, in order to show how the eigenfrequencies depend on the sub-tangential forces and on the rigidity parameters of the constraints at the end of the beam, when various boundary conditions are considered. In section 5, some conclusions are reported.

2. Statement of the problem and calculation of the energetic terms

Consider an elastic column of length L bound through an elastically restrained end in the origin of

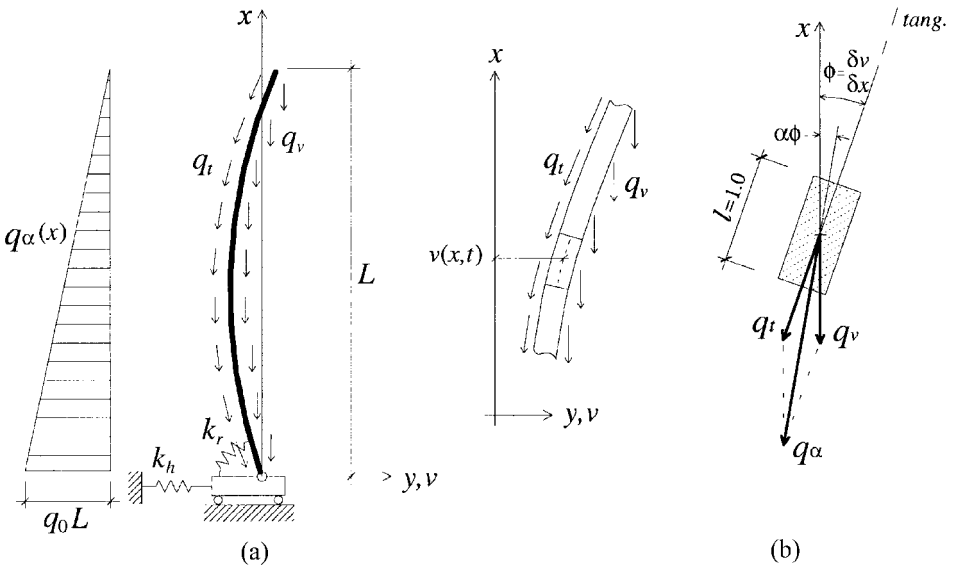

Fig. 1 (a) Column subjected to triangularly distributed subtangential forces in deformed configuration, (b) System of the forces

the reference system, $x = 0$, subjected to distributed sub-tangential forces (Fig. 1). Let the axial component per unit length be denoted by q_v and the tangential force per unit length by q_t. The deflection of the column is assumed to be too small for the behaviour to be governed by Euler's beam theory. For a point at the abscissa x on the beam the deflection is denoted by $v = v(x, t)$, t being the time. For a small deflection, the angle $\phi = \phi(x, t)$ between the x-axis and the tangent to the elastic line can be approximated by $\phi = \partial v / \partial x$. Letting $\alpha\phi$ be the angle between the x-axis and the sub-tangential force q_α, the resultant of q_v and q_t, one easily obtains the relations:

$$\bar{q}_\alpha = \bar{q}_v + \bar{q}_t, \qquad \alpha = \frac{q_t}{q_\alpha} \tag{1}$$

In literature α is known as the non-conservativeness parameter. The use of the parameter α allows one to replace the system of two forces q_v and q_t by one sub-tangential follower force q_α. Once that it is known, by varying the parameter α one can investigate the stability for qualitatively different load conditions. For example, if $\alpha = 0$, the pure axial force applies on the system, while the pure tangential force applies when $\alpha = 1$.

In the present study, as can be noticed in Fig. 1(a), q_α is assumed to be linearly distributed along the x-axis, $q_\alpha(x) = q_0(L - x)$, where $q_0 L$ represents the intensity of q_α at $x = 0$.

The tangential follower forces, q_t, are non-conservative as the resulting virtual work cannot be represented by a potential function. The stability of the system, for various values of the non-conservativeness parameter α and for different values of translational and rotational rigidity of elastic springs k_h and k_r at one end of the beam, respectively, is studied. Various boundary conditions at the other end of the beam will be considered later on. At present, it can be seen that for $k_h \to \infty$ and $k_r \to \infty$ the elastically restrained end becomes a built-in end, which is also termed clamped end. It should be remembered that a built-in end is equivalent to three supports constraints,

located in such a way that the end section of the beam is not capable of undergoing any translation or rotation. When $k_h \to \infty$, that is the translational rigidity parameter becomes greater and greater until approaching infinity, the elastically restrained end can be considered as an elastic hinge with rotational rigidity $k_r \neq 0$. In the particular case of $k_r = 0$ the restrained hinge is usually termed hinged immovable or fixed end support. This type of support possesses only one degree of freedom. For $k_r \to \infty$ and $k_h = 0$, namely when the rotational rigidity approaches infinity and the translational rigidity parameter is zero, the elastically constrained end being considered behaves as an ideal hinge. This type of support is also termed hinge at infinity, sliding hinge, or translational hinge, since the constrained end section can move along the normal to the beam axis. In other words, the end section is fixed against rotation, but free to move in the *y*-direction. Moreover, for $k_r \to \infty$ and $k_h \neq 0$ the end section of the beam is constrained to translate in the y-direction. In this case the reactions of the support are a bending moment and a shear force.

The differential equation describing the flexural displacements of elastic columns can be derived from the energy expression including sub-tangential forces as follows:

$$T = \frac{1}{2}\int_0^L \mu A\left(\frac{\partial v(x, t)}{\partial t}\right)^2 dx \tag{2}$$

$$\Phi_C = \frac{1}{2}\int_0^L EI\left(\frac{\partial^2 v(x, t)}{\partial x^2}\right)^2 dx \tag{3}$$

$$\Phi_H = \frac{1}{2}k_h v^2(0, t) \tag{4}$$

$$\Phi_R = \frac{1}{2}\left(\frac{\partial v(0, t)}{\partial x}\right)^2 = \frac{1}{2}k_r \phi^2(0, t) \tag{5}$$

$$W_c = \frac{1}{2}\int_0^L q_\alpha (L - x)\left(\frac{\partial v(x, t)}{\partial x}\right)^2 dx \tag{6}$$

where T is the kinetic energy, Φ is the elastic potential energy, W_c represents the conservative work. In expressions (3)-(5) the indexes on the left hand stand for column, translational spring and rotational spring, respectively. In the Eqs. (2)-(5) E is the modulus of elasticity, I is the second area moment of inertia, μ is the density, A is the cross-sectional area and k_h, k_r are, as said before, the translational and rotational rigidity of the elastically restrained beam end.

The virtual work of the transverse components of the follower forces δW_{nc} can be expressed as:

$$\delta W_{nc} = -\int_0^L q_t \phi \delta v dx = -\int_0^L q_t \left(\frac{\partial v}{\partial x}\right)\delta v dx = -\int_0^L q_\alpha \alpha \left(\frac{\partial v}{\partial x}\right)\delta v dx \tag{7}$$

Substituting Eqs. (2)-(7) into the extended Hamilton's principle:

$$\delta \int_{t_2}^{t_1} (T - \Phi + W_c) dt + \int_{t_2}^{t_1} \delta W_{nc} dt = 0 \tag{8}$$

after separating variables and rearranging leads to:

$$\int_{t_2}^{t_1}\left\{-\int_0^L \mu A\left(\frac{\partial v}{\partial t}\right)\delta\left(\frac{\partial v}{\partial t}\right)dx-\int_0^L EI\left(\frac{\partial^2 v}{\partial x^2}\right)\delta\left(\frac{\partial^2 v}{\partial x^2}\right)dx+\int_0^L \frac{1}{2}q_\alpha(L-x)\left(\frac{\partial v}{\partial x}\right)\delta\left(\frac{\partial v}{\partial x}\right)dx+\right.$$
$$\left.-\int_0^L q_\alpha \alpha\left(\frac{\partial v}{\partial x}\right)\delta v\,dx-k_h v(0,t)\,\delta v(0,t)-k_r\phi(0,t)\,\delta\phi(0,t)\right\}dt = 0 \qquad (9)$$

It should be noted that in Eq. (8) Φ depicts the sum of Φ_C, Φ_H and Φ_R.

3. Finite element formulation

The total system of length L can be subdivided into n finite elements, whose length is l. Introducing for convenience's sake the following local and adimensional coordinates:

$$\bar{x} = x-(i-1)l, \qquad \eta = \eta(x,t) = \frac{v(x,t)}{l}, \qquad \xi = \frac{\bar{x}}{l} \qquad (10)$$

where i represents the i-th element, Eq. (9) can be written as:

$$\sum_{i=1}^{n}\left\{-\int_0^1 \mu A l^3\left(\frac{\partial^2 \eta}{\partial t^2}\right)\delta\eta\,d\xi-\int_0^1 \frac{EI}{l}\left(\frac{\partial^2 \eta}{\partial \xi^2}\right)\delta\left(\frac{\partial^2 \eta}{\partial \xi^2}\right)d\xi+\int_0^1 \frac{1}{2}q_0 l^3(n-\xi-i+1)^2\left(\frac{\partial \eta}{\partial \xi}\right)\delta\left(\frac{\partial \eta}{\partial \xi}\right)d\xi\right\}+$$

$$-\sum_{i=1}^{n}\left\{\int_0^1 q_0\alpha l^3(n-\xi-i+1)\left(\frac{\partial \eta}{\partial \xi}\right)\delta\eta\,d\xi\right\}-\left|k_h l^2\eta(0,t)\,\delta\eta(0,t)\right|_1-\left|k_r\left(\frac{\partial \eta(0,t)}{\partial \xi}\right)\delta\left(\frac{\partial \eta(0,t)}{\partial \xi}\right)\right|_1 = 0 \qquad (11)$$

In Eq. (11) the subscript 1 represents the first finite element of the system. As can be seen from Fig. 2, the first node of the first finite element is situated at the origin of the reference system. In

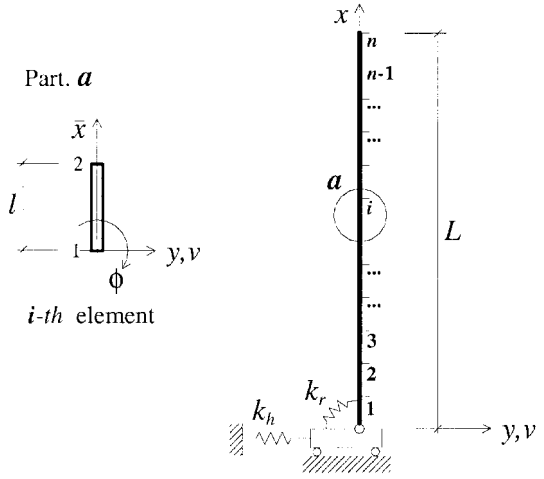

Fig. 2 Discretization of the system into n finite elements

the finite element method, the continuous non-dimensional displacement $\eta = \eta(x, t)$ may be approximated in terms of nodal displacements. The field of lateral displacements can be related to the nodal displacements vector $\boldsymbol{u} = \boldsymbol{u}(t)$ by means of the translational cubic non-dimensional shape functions matrix $\boldsymbol{N} = \boldsymbol{N}(\xi)$, as:

$$\eta(\xi, t) = \boldsymbol{N}^T\boldsymbol{u} = [N_1 \;\; N_2 \;\; N_3 \;\; N_4]\boldsymbol{u} \tag{12}$$

where $\boldsymbol{u} = [v_1 \;\; \phi_1 \;\; v_2 \;\; \phi_2]^T$ and,

$$N_1(\xi) = \frac{1}{l}(1 - 3\xi^2 + 2\xi^3)$$

$$N_2(\xi) = (\xi + 2\xi^2 - \xi^3)$$

$$N_3(\xi) = \frac{1}{l}(3\xi^2 - 2\xi^3)$$

$$N_4(\xi) = (\xi^2 - \xi^3)$$

With the aid of Eq. (12) the discrete dimensionless equation of motion Eq. (11) can be rewritten in terms of nodal displacements in the following synthetic form:

$$\sum_{i=1}^{n} \{-\delta\boldsymbol{u}^T\boldsymbol{m}\ddot{\boldsymbol{u}} - \delta\boldsymbol{u}^T\boldsymbol{k}_e\boldsymbol{u} + \delta\boldsymbol{u}^T\boldsymbol{k}_g\boldsymbol{u} - \delta\boldsymbol{u}^T\boldsymbol{k}_d\boldsymbol{u}\} - \left|\delta\boldsymbol{u}^T\boldsymbol{k}_h\boldsymbol{u}\right|_1 - \left|\delta\boldsymbol{u}^T\boldsymbol{k}_r\boldsymbol{u}\right|_1 = \boldsymbol{0} \tag{13}$$

where $\boldsymbol{m}$ and $\boldsymbol{k}_e$ are the well known mass and elastic rigidity matrices of the Euler beam element, whereas $\boldsymbol{k}_g$ is the geometric rigidity matrix. The translational $\boldsymbol{k}_h$ and rotational $\boldsymbol{k}_r$ rigidity matrices, as well as the non-conservative rigidity matrix $\boldsymbol{k}_d$, of the single finite element, are reported in appendix A. By applying the standard finite element method, the differential equation of motion governing the entire structure can be derived:

$$\boldsymbol{M}\ddot{\boldsymbol{v}} + \boldsymbol{K}_e\boldsymbol{v} - \boldsymbol{K}_g\boldsymbol{v} + \boldsymbol{K}_d\boldsymbol{v} + \boldsymbol{L}^T\boldsymbol{k}_h\boldsymbol{L}\boldsymbol{v} + \boldsymbol{L}^T\boldsymbol{k}_r\boldsymbol{L}\boldsymbol{v} = \boldsymbol{0} \tag{14}$$

where $\boldsymbol{M}$ is the mass matrix of total system, $\boldsymbol{K}_e$ is the elastic rigidity matrix of the system, $\boldsymbol{K}_g$ and $\boldsymbol{K}_d$ are the geometric rigidity matrix and non-conservative rigidity matrix of total system, respectively. In the Eq. (13) $\boldsymbol{v}$ is the global nodal displacement vector and $\boldsymbol{L}$ is the matrix (15) of dimension $4 \times 2(n+1)$ of positioning of the translational and rotational rigidity matrix, $\boldsymbol{k}_h$ and $\boldsymbol{k}_r$, respectively.

$$\boldsymbol{L} = \begin{bmatrix} 1 & 0 & 0 & 0 & \dots & \dots & 0 \\ 0 & 1 & 0 & 0 & \dots & \dots & 0 \\ 0 & 0 & 0 & 0 & \dots & \dots & 0 \\ 0 & 0 & 0 & 0 & \dots & \dots & 0 \end{bmatrix}_{4 \times 2(n+1)} \tag{15}$$

Assuming the solution of Eq. (14) in the form $\boldsymbol{v}(t) = \boldsymbol{V}e^{i\omega t}$ and indicating with $\boldsymbol{K}_T$ the total stiffness matrix, the study of the stability of the system is reduced to the following eigenvalue problem:

$$(\boldsymbol{K}_T - \omega^2\boldsymbol{M})\boldsymbol{V} = \boldsymbol{0} \tag{16}$$

4. Numerical results and discussion

In order to compute the natural frequencies, natural modes and critical distributed sub-tangential forces, the eigenvalues problem associated with the undamped free vibration problem must be solved. The effect of an elastically restrained end on dynamic stability of the beam is taken into account, for various boundary conditions at the other end of the beam. In the following discussion, statically determinate systems will be examined as well as statically indeterminate ones. First, we have considered the effect of the elastically restrained end when the other end is free. Then, the cases in which the second end of the beam was simply supported or bound with a translational support were examined. Finally, a beam fixed at one end and with an elastically restrained support, or with an elastic hinge, at the other end has been analysed.

In order to generate the stability maps and the critical load curves, the dimensionless distributed force parameter $Q = q_0L^4/EI$, the dimensionless eigenfrequency parameter $\Omega = (\mu AL^4\omega^2/EI)^{1/2}$ and the dimensionless parameters of translational and rotational rigidity, $K_h = (k_hL^3/EI)$ and $K_r = (k_rL/EI)$, respectively, are used. It should be kept in mind that when the values of translational and rotational rigidity parameters are assumed $K_h = 10^5$ and $K_r = 10^5$ the end of the beam restrained by elastic spring against rotation and translation can be considered as a totally fixed end.

Given $K_h = 10^5$, Fig. 3 shows the variation of the two lowest values of the eigenfrequency parameter with the sub-tangential force, for various values of the rotational rigidity of the elastically restrained end, when the non-conservativeness parameter is $\alpha = 1.0$. In the case of $\alpha = 1.0$, namely when purely non-conservative forces are applied to the systems, flutter-type instability occurs for all values of the rotational rigidity parameter K_r. As is well known, flutter type instability takes place when the two lowest frequencies, ω_1 and ω_2, meet each other. The value of the parameter Q at which the two lowest frequencies become complex conjugate is the critical flutter value of the distributed sub-tangential force. Fig. 3 shows that also for a very small value of the rotational rigidity of the elastically restrained end, when the system is subjected to a distribution of circulatory load, the instability for flutter takes place with a non void value of the critical load. In other words, the coalescence of the first two frequencies is always observed in Fig. 3.

Fig. 4 presents the eigenfrequencies curves for various values of the translational rigidity K_h when the non-conservativeness parameter $\alpha = 1.0$ and the rotational rigidity parameter is $K_r = 10^5$. In this case, where an elastically translational ideal hinge at the left end of the beam is considered, all the observations referring to the curves plotted in Fig. 3 could be repeated in Fig. 4 for various values of the translational rigidity.

Figs. 5 and 6 show the same analysis for the second boundary condition, that is when the right end of the beam is simply supported. Fig. 5 also shows, through the eigenfrequencies curves, the development of the phenomenon of passage of type-instability. It can be seen that, for growing values of the translation rigidity parameter K_r, the system that was unstable for divergence, becomes unstable for flutter with an increase of the critical load.

The type of instability depends on the values of the rigidity parameter: the divergence occurs only for $K_r \leq 10^0$ and the flutter occurs only for $K_r \geq 10^1$. When $K_r = 10^5$ is considered (Fig. 6), the divergence-type instability is shown for $K_r \leq 10^1$ and the flutter-type is depicted for $K_r \geq 10^2$. As is well known, the divergence type instability takes place when the smallest frequency of the system ω_1 assumes void value. The value of the parameter Q at which the first frequency ω_1 becomes void is the critical divergence value of the distributed sub-tangential force.

For others boundary conditions, corresponding to $\alpha = 1.0$, the eigenfrequencies curves are illustrated in Fig. 7 and Fig. 8 when the second end is bound through an ideal hinge and in Fig. 9 and Fig. 10 when the second extreme is clamped. Through these curves the instability, which is underlined for flutter and for divergence, comes to depend on the values of the rigidity parameters of translation and rotation of the elastic constraints, located at the left end of the beam, as well as on the typology of the boundary at the right end of the beam. It should be noted that the results shown from Fig. 3 to Fig. 10, were worked out always assuming the non-conservativeness parameter $\alpha = 1.0$, that is only a purely circulatory load has been considered.

In order to show the effect of the non-conservativeness parameter on the behaviour of the system, now the curves of the critical load will be investigated for $0.0 \le \alpha \le 1.0$. For the beam connected to a rotational elastic hinge (when the translational spring constant is $K_h = 10^5$) at the left end, the critical load curves for different values of the parameter α are brought in Fig. 11 as a function of the rigidity parameter K_r. The curves corresponding to the values of $\alpha \le 0.4$ are always representative of a divergence instability type. The critical load grows when greater values of α and of the rotational rigidity of the elastically restrained end K_r of the beam are considered. The curves for $0.5 \le \alpha \le 0.9$, show that for low values of K_r the system loses stability in the form of the divergence, but for increasing values of K_r the curves introduce a change of unstable form as well as a jump in the value of the critical load. Therefore, for determined values of the rotational rigidity of the elastically restrained end, the system becomes unstable for flutter once the value of the critical load has been reached. It should be noted that for $\alpha = 1.0$, the system also introduces an elevated value of critical load for a null rotational rigidity, according to what has been seen in Fig. 3.

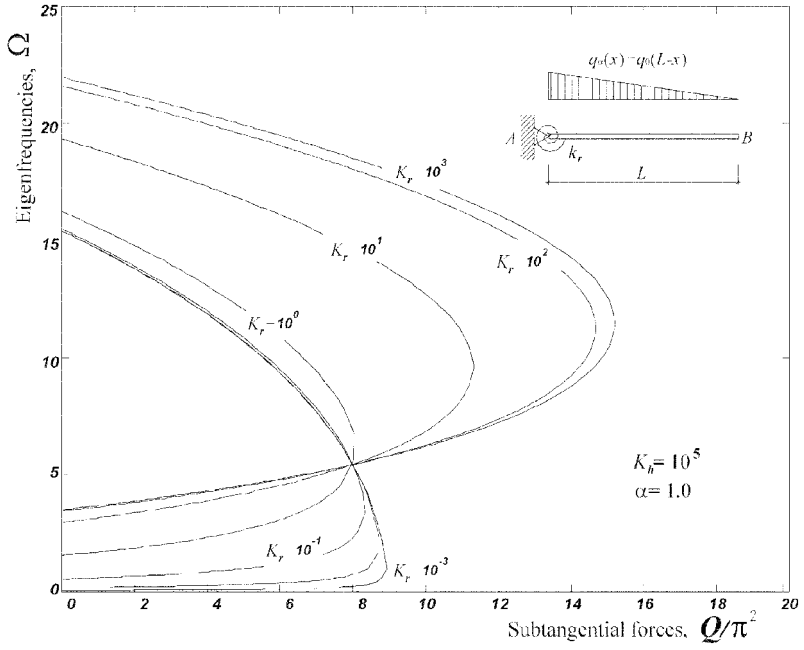

Fig. 3 Eigenfrequency curves for a cantilever beam and for various values of rotational rigidity parameter K_r, when $K_h = 10^5$ and $\alpha = 1.0$

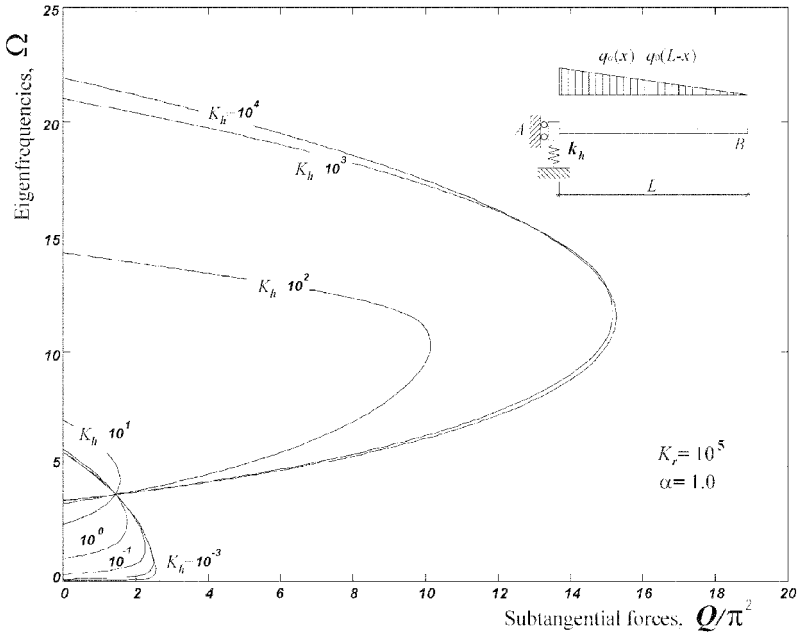

Fig. 4 Eigenfrequency curves for a cantilever beam and for various values of translation rigidity parameter K_h, when $K_r = 10^5$ and $\alpha = 1.0$

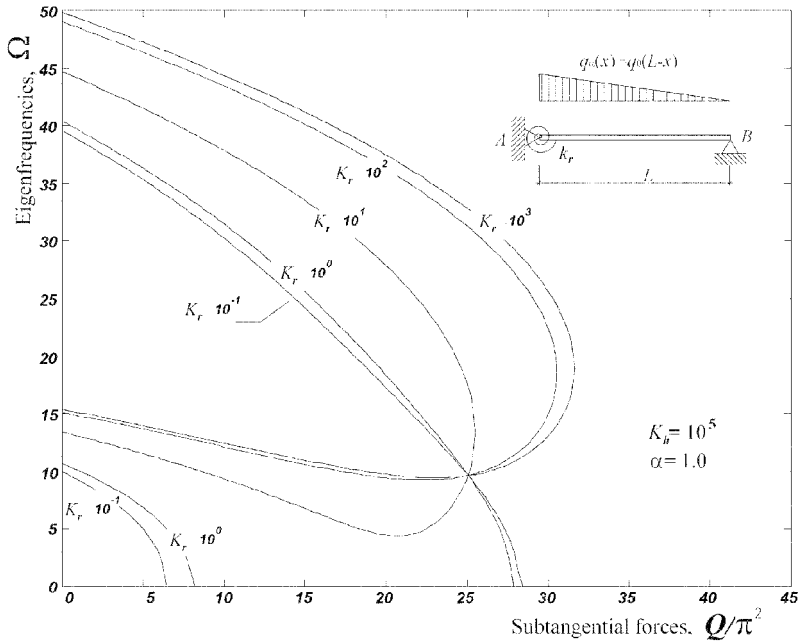

Fig. 5 Eigenfrequency curves for a simply supported beam and for various values of rotational rigidity parameter K_r, when $K_h = 10^5$ and $\alpha = 1.0$

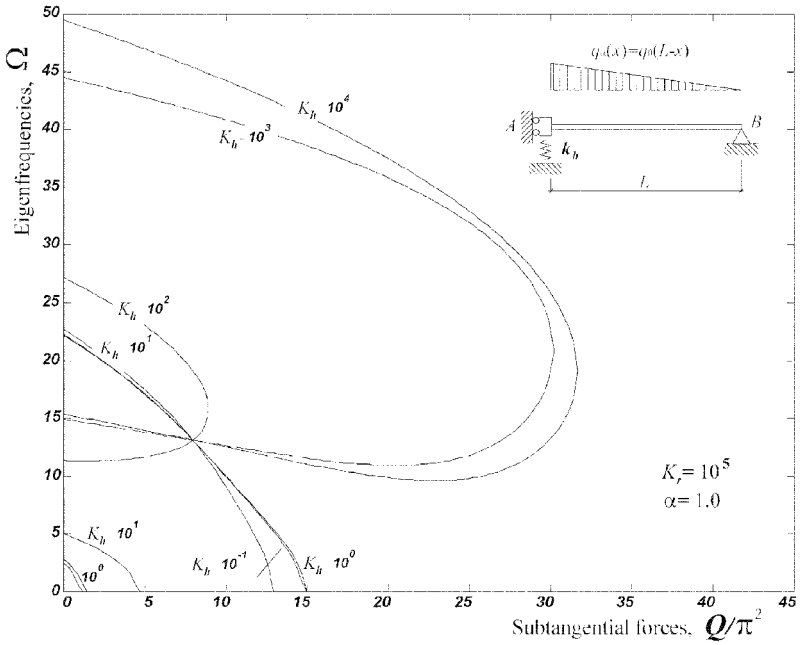

Fig. 6 Eigenfrequency curves for a simply supported beam and for various values of translation rigidity parameter K_h, when $K_r = 10^5$ and $\alpha = 1.0$

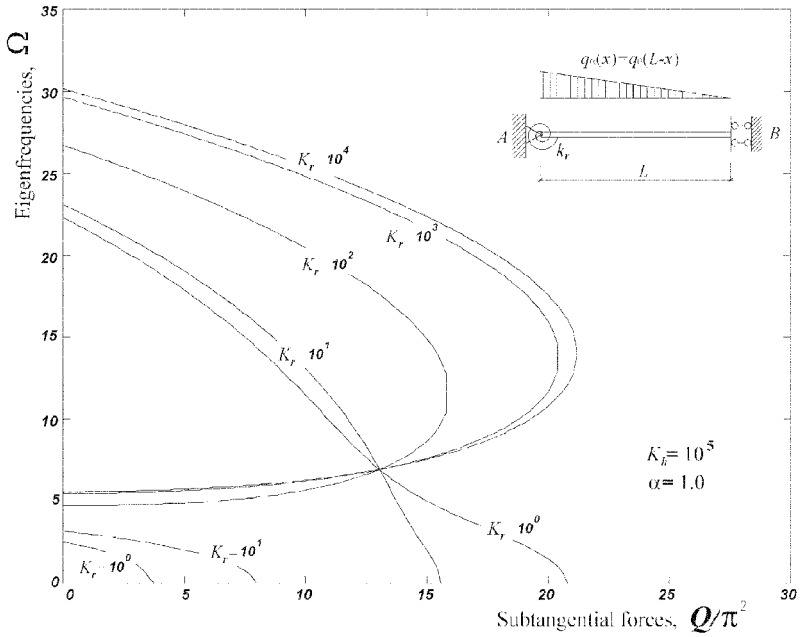

Fig. 7 Eigenfrequency curves for a beam with the second end bound through a sliding hinge, for various values of rotational rigidity parameter K_r, when $K_h = 10^5$ and $\alpha = 1.0$

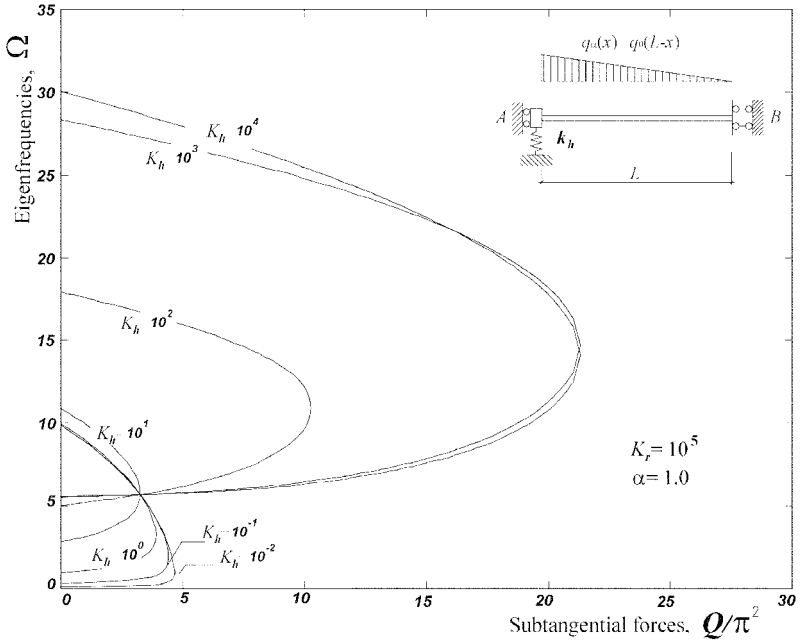

Fig. 8 Eigenfrequency curves for a beam with the second end bound through a sliding hinge, for various values of translational rigidity parameter K_h, when $K_r = 10^5$ and $\alpha = 1.0$

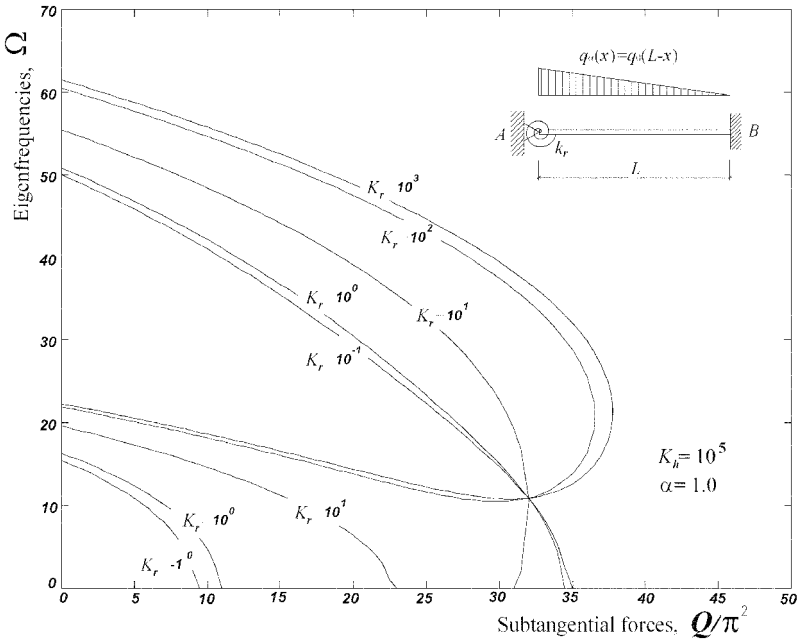

Fig. 9 Eigenfrequency curves for a beam with the second end clamped, for various values of rotational rigidity parameter K_r, when $K_r = 10^5$ and $\alpha = 1.0$

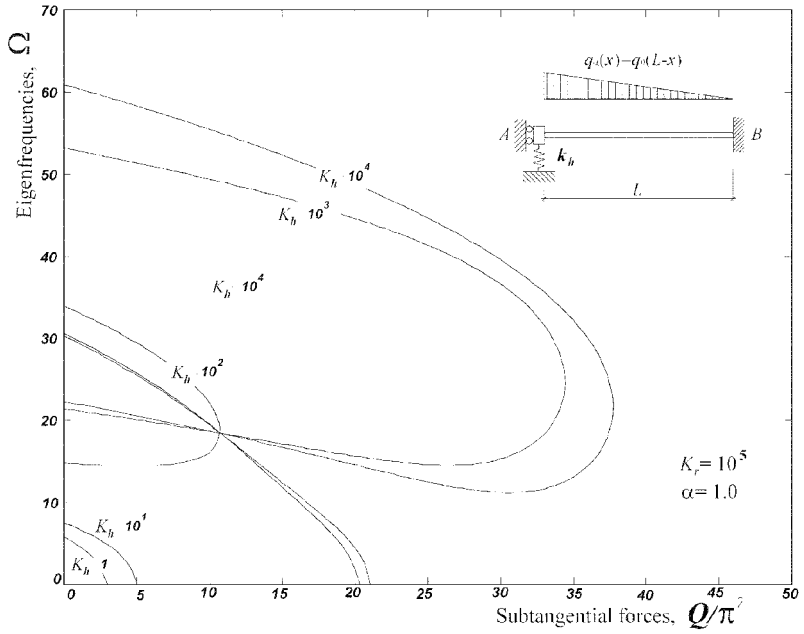

Fig. 10 Eigenfrequency curves for a beam with the second end clamped, for various values of translation rigidity parameter K_h, when $K_r = 10^5$ and $\alpha = 1.0$

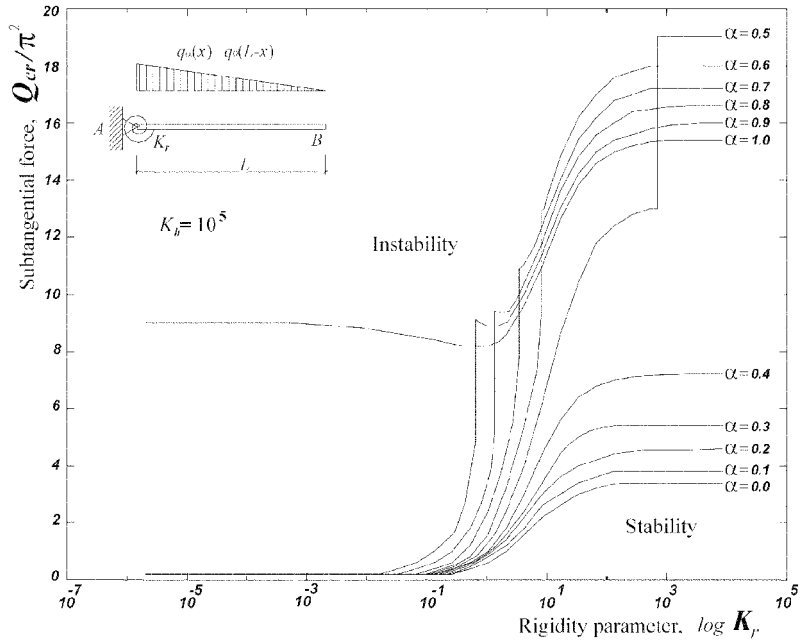

Fig. 11 Critical load curves for a cantilever beam and for different values of the non-conservativeness parameter α, when $K_h = 10^5$

Fig. 12 shows the critical load of the system as a function of K_h, when $\alpha = 1.0$ and $K_r = 10^5$. In this case, as well as for the two next systems, the ideal hinge located at the left-hand end is elastically restrained against translation. A peak in the value of the critical load is shown, in correspondence of a specific value of the parameter of rigidity K_h. It can be seen from Fig. 12 how the peak value of the critical load turns out to be greater than the one corresponding to the system bound through a fixed hinge. In condition of incipient instability by flutter, when a removal of the system from the *x*-axis is considered, an increase of the value of the normal components of load will be produced. In the case of an immovable hinge where any translation of the left end of the beam is prevented, a vibration of increasing amplitude can occur under the constant value of the critical load, so that the flutter instability can be produced. In the case of Fig. 12, instead, the elastically restrained end allows the system to translate in the *y* direction and the dynamic phenomenon of vibration turns out to be instability by divergence, for values of the applied load greater than the value of the critical load.

The jump phenomenon is also represented in Fig. 13, where the eigenfrequencies curves are shown for various values of the translational rigidity parameter K_h, when $K_r = 10^5$ and $\alpha = 1$.

From Fig. 14 to Fig. 20 the sub-tangential forces are shown as a function of a rigidity parameter, for various boundary conditions. From Fig. 14 it can be seen how the phenomenon of jump of the critical load occurs only for the values of $\alpha = 0.75$ and $\alpha = 1.0$. For the lowest determinations of the parameter, that is for $\alpha = 0.0$ and $\alpha = 0.25$, the system becomes unstable always for divergence. Moreover, for $\alpha = 0.0$ the value of the critical load is independent from the value of the rigidity parameter of the elastically restrained end. It should be noted that, for elevated values of translation rigidity, the system reduces to a cantilever beam and the value of the critical load depends on the degree of non-conservativeness of the applied load.

Figs. 15-16 show the effect of the non-conservativeness parameter α on the critical load. The beam is simply supported at the right-hand end whereas at the other end it is elastically restrained against rotation and against translation, respectively. Fig. 15 shows that, for $0.0 \le \alpha \le 0.7$, the instability of the system is always of a divergence type, and the critical load grows for increasing values of the parameter α. It is worth noting that, in the case of $0.8 \le \alpha \le 1.0$, the system introduces the passage of unstable form, from divergence to flutter with a jump in the critical load. When instability is in the form of flutter, the critical load decreases with increasing values of α. From Fig. 16, it can be seen that the only curve of critical load that does not show any passage of unstable form corresponds to $\alpha = 0.0$. For this value of the non-conservativeness parameter the system becomes unstable for divergence for all the values of the translation rigidity.

For $0.1 \le \alpha \le 0.7$, instead, the system shows two passages of unstable form, from divergence to flutter and return to the divergence, as a function of the translation rigidity parameter K_h. Finally, for $0.8 \le \alpha \le 1.0$, only the passage from divergence to flutter is shown. The critical load curves illustrated in Figs. 17-20 refer to beams which are elastically restrained at the right-hand end and constrained by an ideal hinge or totally fixed at the other end.

It is worth while noting that numerical simulations performed for different boundary conditions of the beam, as well as for various values of the rigidity parameters to the rotation and to the translation, reveal their influence on the type of instability and on the value of the critical load for each value of the α parameter. The above numerical results and diagrams have been computed using PC-Matlab.

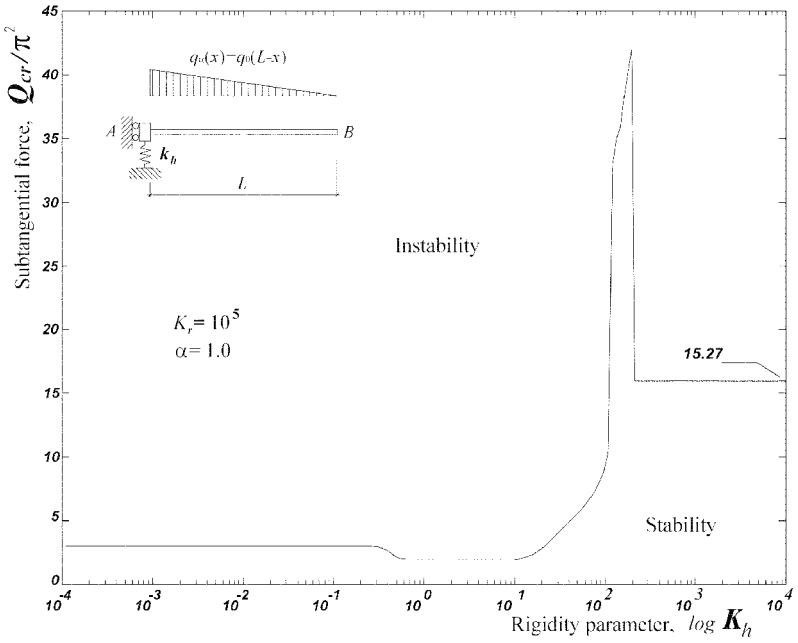

Fig. 12 Sub-tangential force versus translational rigidity parameter K_h, for $K_r = 10^5$ and $\alpha = 1.0$

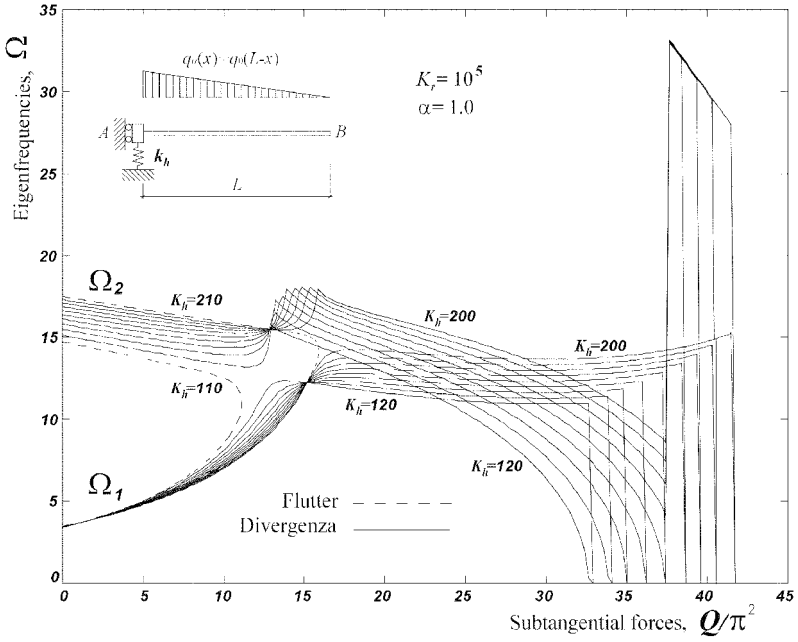

Fig. 13 Eigenfrequency curves for a cantilever beam for various values of translational rigidity parameter K_h, when $K_r = 10^5$ and $\alpha = 1.0$, showing the passage of unstable form from flutter to divergence

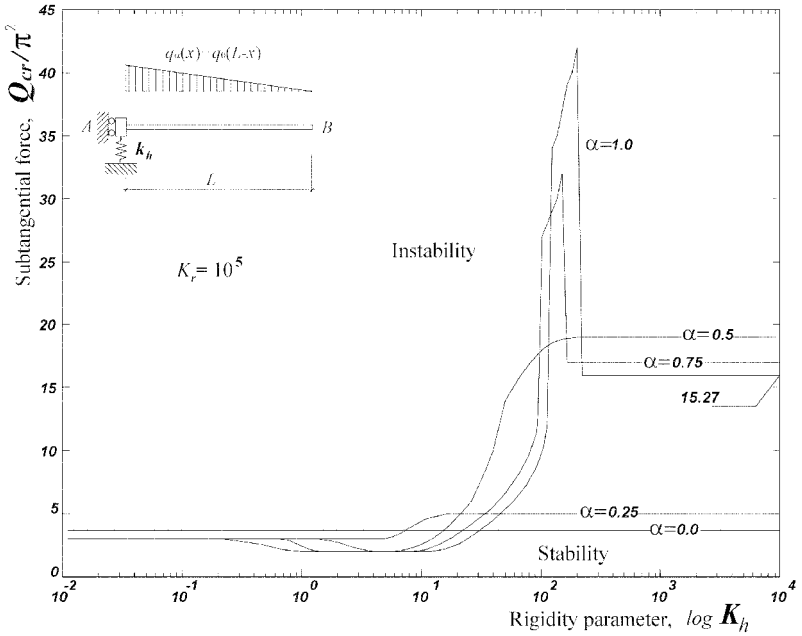

Fig. 14 Sub-tangential force versus translational rigidity parameter K_h, for $K_r = 10^5$, when five values of non-conservativeness parameter α are considered

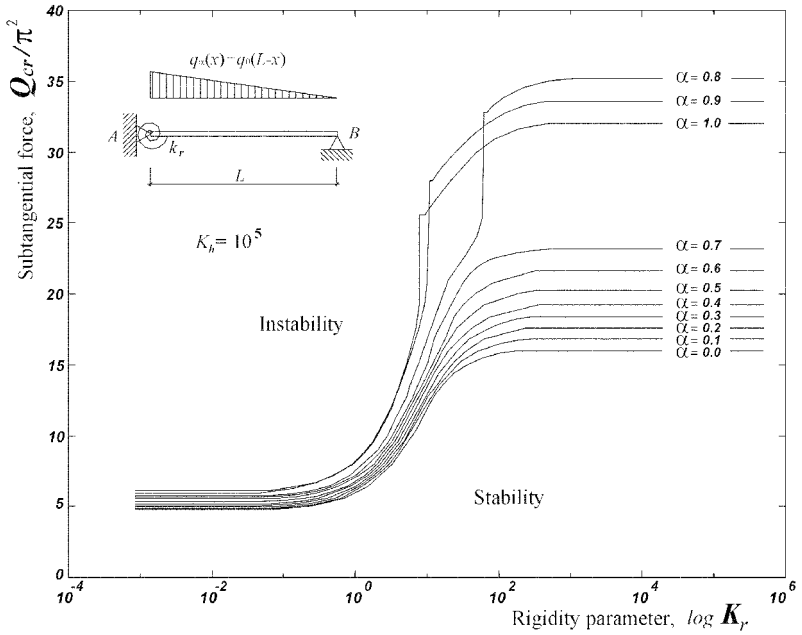

Fig. 15 Sub-tangential force versus the rotational rigidity parameter K_r, for various values of non-conservativeness parameter α, when the first end of the beam is constrained by an elastic hinge and the second one is simply supported

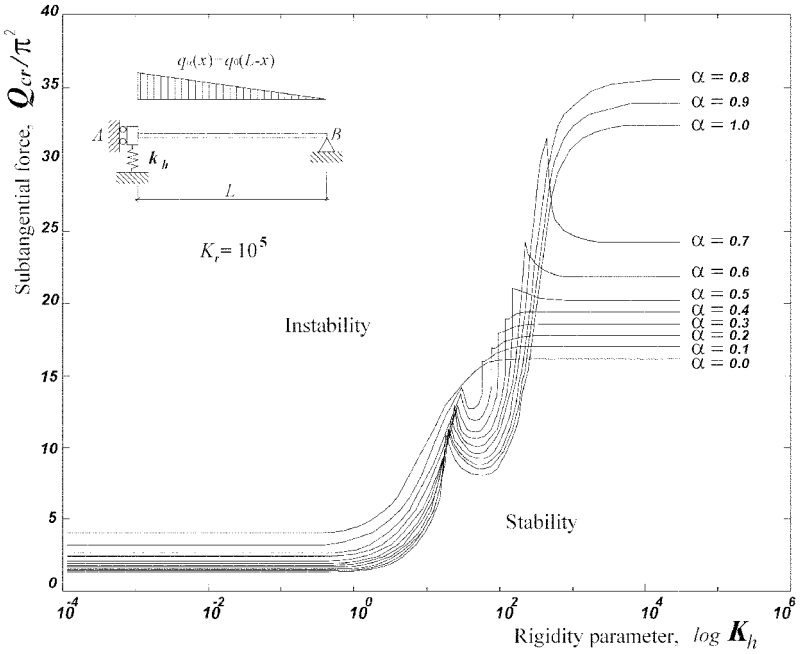

Fig. 16 Sub-tangential force versus the rotational rigidity parameter K_r, for various values of α, when the first end of the beam is constrained by an elastic spring and the second one is simply supported

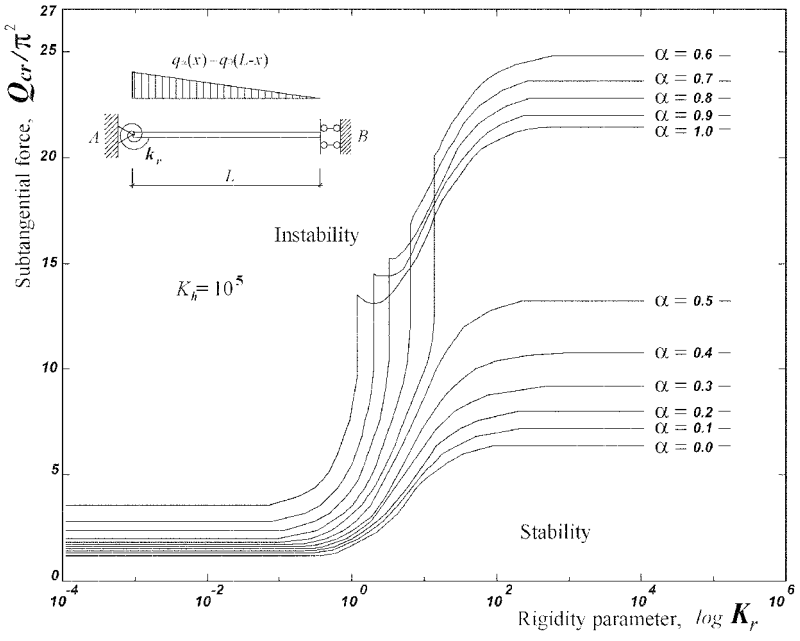

Fig. 17 Critical load curves for various values of the parameter α when the first end of the beam is constrained by an elastic hinge and the second one is bound with an ideal hinge

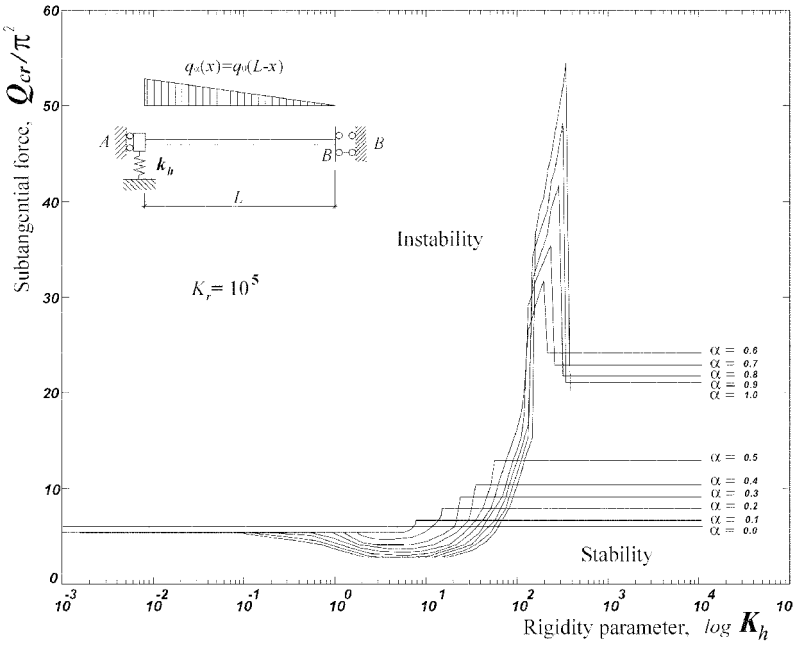

Fig. 18 Critical load curves for various values of the parameter α when the first end of the beam is constrained by an elastic spring and the second one is bound through an ideal hinge

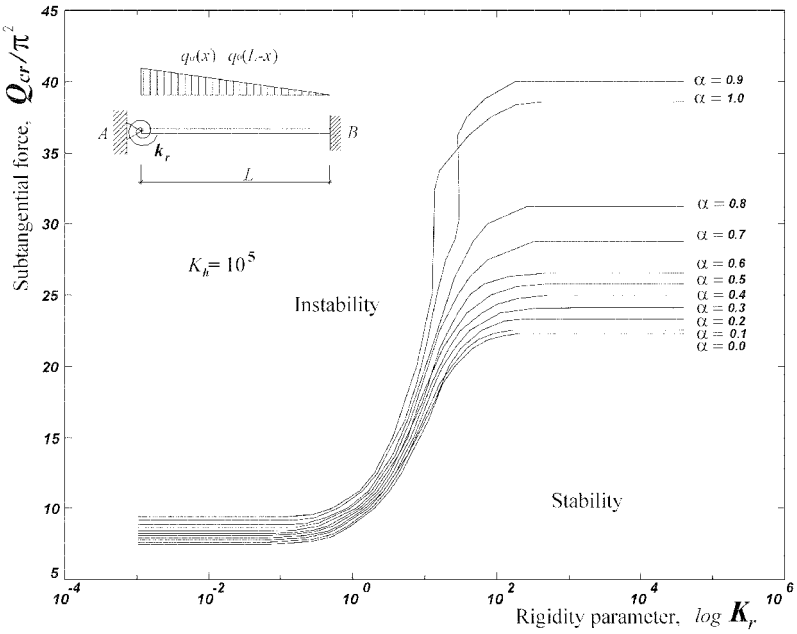

Fig. 19 Critical load curves versus the rotational rigidity parameter K_r when the first end of the beam is constrained by an elastic hinge and the second end is fixed

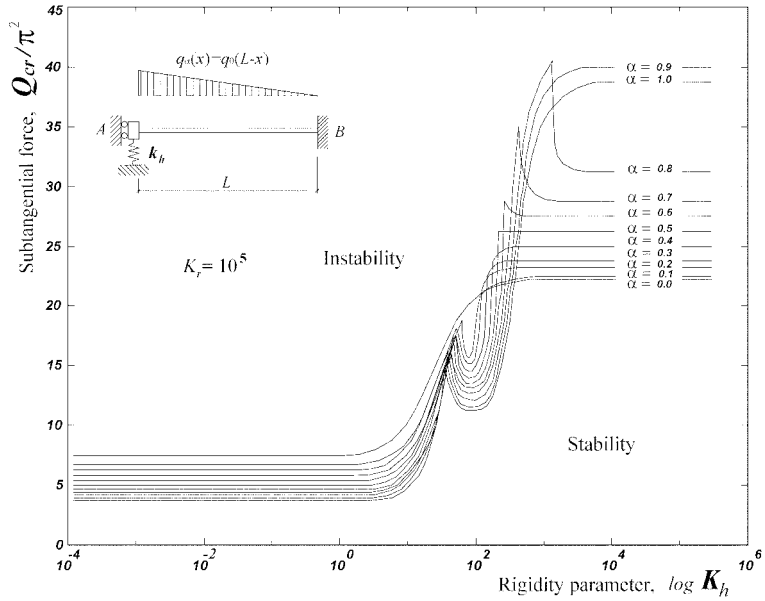

Fig. 20 Critical load curves versus the translational rigidity parameter K_h when the first end of the beam is constrained by an elastic spring and the second one is fixed

5. Final observations and conclusions

In this paper, a finite element procedure for prismatic beams, under conservative and non-conservative forces has been developed. The influence of the degree of non-conservativeness of the load on the eigenfrequency curves is also shown for various boundary conditions. The main innovation introduced by the present work regards the effect of an elastically restrained end on the dynamic stability of elastic prismatic beams under triangularly distributed sub-tangential forces. At the ends of the beams various fixed and movable supports have been considered. In particular, an analysis has been undertaken of the influence of fixed elastic hinges and translational hinges constrained by linear elastic springs located at the left-hand ends of the beams.

It is worth nothing that a translational hinge may be represented by two parallel bars with hinges at their extremities, or by two hinges and a rigid movable plate. In the case of parallel bars, each bar with its hinges is usually termed pendulum support. At one end of the bars the hinges are fixed to the ground. At the other end of the two parallel bars the hinges are fixed to a movable plate. So far in this discussion, the axes of the pendulums have been considered to be parallel to the initial configuration of the beams. It may be observed that the number of bars is equal to the number of parameters determining completely the reactions at this constraint.

It should be noted that the choice of a structural model depends on the purpose of the investigation. Actually, elastic beams are three dimensional continua but, for certain classes of their possible motions, they can be modelled at a simpler level. In the present work the one-dimensional theory for the flexural motion of Bernoulli-Euler beam has been employed. The F.E. model used to study the dynamic stability of beams under conservative and non-conservative forces consists of beam elements.

As is well known, the equation of motion in matrix form for a beam subjected to a sub-tangential follower load is different from the equation of motion of a beam subjected to a conservative axial load. One can easily identify the nature of the non-conservative system by the presence of a non-symmetric matrix in the equation of motion. In fact, when the loading is conservative for $\alpha = 0$, the matrix of non-conservative rigidity $\boldsymbol{k}_d$ is a null matrix. This matrix $\boldsymbol{k}_d$, which accounts for non-conservative forces of circulatory type, is denoted in the literature as load correction matrix or load behaviour matrix. Since circulatory forces do not derive from a potential, the load correction stiffness matrix is, in general, non-symmetrical.

The present approach can be extended to situations in which coupling between the various forms of motion such as bending, shear and torsion takes place.

Acknowledgements

This research was supported by the Italian Ministry for University and Scientific, Technological Research MIUR (40 and 60%). The research theme is one of the subjects of the Centre of Study and Research for the Identification of Materials and Structures (CIMEST) - M. Capurso. The writers are grateful to the reviewers for their useful comments.

References

Argyris, J.H. and Symeonidis, Sp. (1981), "Nonlinear finite element analysis of elastic systems under non-conservative loading-natural formulation. Part. I Quasistatic problems", *Comput. Meth. Appl. Mech. Eng.*, **26**, 75-123.

Beck, M. (1952), "Die Knicklast des einseitig eingespannten, tangential gedruckten Stabes", *Z. Angew. Math. Phys.*, **3**, 225-228.

Bolotin, V.V. (1965), *Non-conservative Problems of the Theory of Elastic Stability*, Pergamon Press, London.

De Rosa, M. and Franciosi, C. (1990), "The influence of an intermediate support on the stability behaviour of cantilever beams subjected to follower forces", *J. Sound Vib.*, **137**(1), 107-115.

Glabisz, W. (1999), "Vibration and stability of a beam with elastic supports and concentrated masses under conservative and non-conservative forces", *Comput. Struct.*, **70**, 305-313.

Kounadis, A.N. (1983), "The existence of regions of divergence instability for non-conservative systems under follower forces", *Int. J. Solids Struct.*, **19**(8), 725-733.

Lee, H.P. (1995), "Dynamic stability of a rod with an intermediate spring support subject to sub-tangential follower forces", *Comput. Meth. Appl. Mech. Eng.*, **125**, 141-150.

Leipholz, H. (1980), *Stability of Elastic Systems*, Sijthoff-Noordhoff, The Netherlands.

Leipholz, H. and Bhalla, K. (1977), "On the solution of the stability problems of elastic rods subjected to triangularly distributed tangential follower forces", *Ingenieur-Archiv*, **46**, 115-124.

Liebowitz, H., Vanderveldt, H. and Harris, D.H. (1967), "Carrying capacity of notched column", *Int. J. Solids Struct.*, **3**, 489-500.

Marzani, A. and Viola, E. (2002), "Influenza dell'incastro elasticamente cedevole sulla instabilità dinamica per flutter e per divergenza di una colonna", Nota tecnica n.61 DISTART, University of Bologna, Italy.

Mote, Jr. (1971), "Non-conservative stability by finite elements", *J. Eng. Mech. Div.*, EM3, 645-656.

Ryu, B.J., Sugiyama, Y., Yim, K.B. and Lee, G.S. (2000), "Dynamic stability of an elastically restrained column subjected to triangularly distributed sub-tangential force", *Comput. Struct.*, **76**, 611-619.

Sugiyama, Y. and Kawagoe, H. (1975), "Vibration and stability of elastic columns under the combined action of uniformly distributed vertical and tangential forces", *J. Sound Vib.*, **38**(4), 341-355.

Sugiyama, Y. and Mladenov, K.A. (1983), "Vibration and stability of elastic columns subjected to triangularly

distributed sub-tangential forces", *J. Sound Vib.*, **88**(4), 447-457.
Viola, E., Nobile, L. and Marzani, A. (2002), "Boundary conditions effect on the dynamic stability of beams subjected to triangularly distributed sub-tangential forces", *Proc. of the Second Int. Conf. on Advantages in Structural Engineering and Mechanics (ASEM'02)*, 21-23 August 2002, Busan, Korea.
Ziegler, H. (1977), *Principles of Structural Stability*, Birkhäuser, Basel/Stuttgart.

Appendix A

The matrix of geometric rigidity is symmetric and depends on the index i which concerns the generic beam finite element

$$\boldsymbol{k}_g = \frac{1}{2}q_0 l^3 \begin{bmatrix} a & b & c & e \\ & f & g & o \\ & & p & r \\ & & & s \end{bmatrix}$$

where:

$$a = \frac{6}{5l^2}\left(n^2 + i^2 - 2ni + n - i + \frac{2}{7}\right) \qquad b = -\frac{1}{10l}\left(n^2 + i^2 - 2ni - \frac{2}{7}\right)$$

$$c = -\frac{6}{5l^2}\left(n^2 + i^2 - 2ni + n - i + \frac{2}{7}\right) \qquad e = -\frac{1}{10l}\left(n^2 + i^2 - 2ni + 2n - 2i + \frac{5}{7}\right)$$

$$f = \frac{1}{15}\left(2n^2 + 2i^2 - 4ni + 3n - 3i + \frac{9}{7}\right) \qquad g = \frac{1}{10l}\left(n^2 + i^2 - 2ni - \frac{2}{7}\right)$$

$$o = -\frac{1}{30}\left(n^2 + i^2 - 2ni + n - i + \frac{3}{7}\right) \qquad p = \frac{6}{5l^2}\left(n^2 + i^2 - 2ni + n - i + \frac{2}{7}\right)$$

$$r = \frac{1}{10l}\left(n^2 + i^2 - 2ni + 2n - 2i + \frac{5}{7}\right) \qquad s = \frac{1}{15}\left(2n^2 + 2i^2 - 4ni + n - i + \frac{2}{7}\right)$$

The matrix of non-conservative rigidity is non-symmetric and also depends on the index i:

$$\boldsymbol{k}_d = q_0 \alpha l^3 \begin{bmatrix} \overline{a} & \overline{b} & \overline{c} & \overline{d} \\ \overline{e} & \overline{f} & \overline{g} & \overline{i} \\ \overline{l} & \overline{m} & \overline{n} & \overline{o} \\ \overline{p} & \overline{q} & \overline{r} & \overline{s} \end{bmatrix}$$

where:

$$\overline{a} = -\frac{6}{l^2}\left(\frac{n}{12} - \frac{i}{12} + \frac{11}{210}\right) \qquad \overline{b} = \frac{1}{10l}\left(-n + i - \frac{23}{21}\right)$$

$$\overline{c} = \frac{6}{l^2}\left(\frac{n}{12} - \frac{i}{12} + \frac{11}{210}\right) \qquad \overline{d} = \frac{1}{10l}\left(n - i + \frac{31}{42}\right)$$

$$\overline{e} = \frac{1}{10l}\left(n - i + \frac{12}{21}\right) \qquad \overline{f} = \frac{1}{210}$$

$$\overline{g} = \frac{1}{10l}\left(-n + i - \frac{12}{21}\right) \qquad \overline{i} = \frac{1}{60}\left(-n + i - \frac{5}{7}\right)$$

$$\bar{l} = \frac{6}{l^2}\left(-\frac{n}{12}+\frac{i}{12}-\frac{13}{420}\right) \qquad \bar{m} = \frac{1}{10l}\left(n-i+\frac{11}{42}\right)$$

$$\bar{n} = \frac{6}{l^2}\left(\frac{n}{12}-\frac{i}{12}+\frac{13}{420}\right) \qquad \bar{o} = \frac{1}{10l}\left(-n+i+\frac{2}{21}\right)$$

$$\bar{p} = \frac{1}{10l}\left(-n+i-\frac{3}{7}\right) \qquad \bar{q} = \frac{1}{60}\left(n-i+\frac{2}{7}\right)$$

$$\bar{r} = \frac{1}{10l}\left(n-i+\frac{3}{7}\right) \qquad \bar{s} = \frac{1}{210}$$

The matrices of translation rigidity $\boldsymbol{k}_h$ and rotational rigidity $\boldsymbol{k}_r$, are independent from the index i, so they take on the following aspects:

$$\boldsymbol{k}_h = k_h l^2 \begin{bmatrix} 1 & 0 & 0 & 0 \\ 0 & 0 & 0 & 0 \\ 0 & 0 & 0 & 0 \\ 0 & 0 & 0 & 0 \end{bmatrix}; \qquad \boldsymbol{k}_r = k_r \begin{bmatrix} 0 & 0 & 0 & 0 \\ 0 & 1 & 0 & 0 \\ 0 & 0 & 0 & 0 \\ 0 & 0 & 0 & 0 \end{bmatrix};$$

Notation

q_v	: unidirectional component per unit length of the sub-tangential force
q_t	: tangential force per unit length
q_α	: sub-tangential force
x	: coordinate of reference
v	: beam deflection
ϕ	: angle between the x-axis and the tangent to the elastic line
α	: non-conservativeness parameter
L	: total length of the beam
T	: kinetic energy
Φ_C	: elastic potential energy of the column
Φ_H	: elastic translational energy of the elastically restrained end
Φ_R	: elastic rotational energy of the elastically restrained end
W_c	: conservative work
δW_{nc}	: non-conservative virtual work
t	: time
μ	: density
A	: cross-sectional area
E	: Young's elasticity modulus
I	: second area moment of inertia
i	: index of position of the generic finite element
l	: length of the finite element
$\bar{x}$	: local coordinate for the generic finite element
η	: normalized variable of configuration
ξ	: adimensional local coordinate for the generic finite element
N_i	: adimensional shape functions
$\boldsymbol{u}$	: vector of nodal displacements
$\boldsymbol{N}$	: matrix of the adimensional shape functions $N_i(\xi)$
$\boldsymbol{m}$	: mass matrix of the single finite element
$\boldsymbol{k}_e$	: matrix of elastic rigidity of the single finite element
$\boldsymbol{k}_g$	: matrix of geometric rigidity of the single finite element

$\boldsymbol{k}_d$: matrix of non-conservative rigidity of the single finite element
$\boldsymbol{k}_h$: matrix of translational rigidity of the elastic spring concerning the first finite element
$\boldsymbol{k}_r$: matrix of rotational rigidity of the elastic hinge concerning the first finite element
$\boldsymbol{M}$: matrix of mass of total system
$\boldsymbol{K}_e$: matrix of elastic rigidity of total system
$\boldsymbol{K}_g$: matrix of geometric rigidity of total system
$\boldsymbol{K}_d$: matrix of non-conservative rigidity of total system
$\boldsymbol{v}$: global nodal displacements vector of the system
$\boldsymbol{L}$: localisation matrix with dimension $4\times2(n+1)$ containing only 1 and 0
$\boldsymbol{V}$: modal shape
ω : eigenfrequency
$Q = q_0L^4/EI$: load parameter
$\Omega = (\mu AL^4\omega^2/EI)^{1/2}$: eigenfrequency parameter
$K_h = (k_hL^3/EI)$: translational rigidity parameter
$K_r = (k_rL/EI)$: rotational rigidity parameter